Life Sciences 239 (2019) 116868

Contents lists available at ScienceDirect

Life Sciences

journal homepage: www.elsevier.com/locate/lifescie

The therapeutic effect of dexmedetomidine on protection from renal failure via inhibiting KDM5A in lipopolysaccharide-induced sepsis of mice

Yan Liu[a,b,1], Yanming Yu[c,1], Jicheng Zhang[a,**], Chunting Wang[a,*]

[a] Department of Critical Care Medicine, Shandong Provincial Hospital Affiliated to Shandong University, Jinan, Shandong, 250000, China
[b] Department of Infectious Disease, The Affiliated Yantai Yuhuangding Hospital of Qingdao University Institution, Yantai, Shandong, China
[c] Department of Nephrology, The Affiliated Yantai Yuhuangding Hospital of Qingdao University, Yantai, Shandong, 264000, China

ARTICLE INFO

Keywords:
Sepsis
Renal failure
DEX
H3K4me3
KDM5A

ABSTRACT

Background: Sepsis is an inflammatory response undergoing the complicate pathophysiological changes for host defense against pathogens. Previous studies suggested that dexmedetomidine (DEX) was served to controlling the over-reactive inflammatory effects to protect from the sepsis-induced organ failure via modulating histone methylation. However, the genome-wide changes of histone methylations upon DEX for sepsis treatment were poorly explored.

Materials and methods: The acute kidney injury (AKI) mouse model were induced by lipopolysaccharide (LPS). DEX and KDM5 (H3K4 demethylases) inhibitors were used to add additionally. H3K4me3 antibody was used to conduct the ChIP-seq assay in renal cortex tissues.

Results: We observed that the overall H3K4me3 levels were obviously declined in AKI group compared to the normal control. We further observed that the therapeutic effect of DEX was basically equal with CPI-455 and KDM5A–IN–1 but better than PBIT. The overall H3K4me3 level was reduced in AKI group compared to DEX ($p = 0.008$), and KDM5A–IN–1 groups ($p = 0.022$). The H3K4me3 enrichment of the multiple genes associated with inflammatory cytokines such as TNF-α, NOS2 and CCL2 increased in AKI model, but decreased upon DEX or KDM5A–IN–1 treatment. Consistently, transcription and protein levels of genes such as TLR4, MYD88, MTA1, PTGS2, CASP3 associated with NF-κB signaling pathway were all compromising after treated with DEX or KDM5A–IN–1 groups compared to AKI group.

Conclusion: Taken together, our data determined that DEX could attenuate AKI through KDM5A inhibition in sepsis.

1. Background

Sepsis is an overwhelming systemic inflammatory response to bacterial invasion with 3% morbidity and 25% mortality rates as well as 80% mortality of the concurrent septic shock [1,2]. Sepsis-related multi-organ failure remains the major cause of death in the intensive care unit. Kidney is one of the most susceptible organs to damage among sepsis patients, in whom more than 50% develop an acute kidney injury (AKI) and the mortality rate can be as high as 60% [3,4]. The pathogenesis of septic AKI is complicate, including renal macro- and micro-circulatory disturbance, over-reactive inflammatory, oxidative stress, coagulation cascade activation, and imbalanced energy metabolism [5].

Despite the increasingly deep understanding of these pathophysiologic processes, the septic AKI treatment is still beyond satisfaction. Thus, exploring effective therapeutic approaches for septic AKI is necessary. Dexmedetomidine (DEX) as a highly selective α2-adrenoreceptor agonist [6], has been utilized as adjunctive therapy in patients with sepsis through the pro-inflammatory response down-regulation and the anti-inflammatory response controlling. Previous studies revealed one of the rational for DEX was that DEX could inhibit histone deacetylases (HDACs) such as HDAC2 and HDAC5 as well as maintain histone stability [7,8], to modulate the chromatin structure and gene transcription [9]. Furthermore, besides HDACs, histone demethylases were also reported to play an important role in organ protection and epigenetic control of inflammatory response in sepsis recently [10–13].

* Corresponding author. Department of Critical Care Medicine, Shandong Provincial Hospital Affiliated to Shandong University, No. 324 Jingwu Road, Jinan, Shandong, 250000, China
** Corresponding author.
E-mail addresses: jczhangicu@163.com (J. Zhang), wangchuntingicu@163.com (C. Wang).
[1] Authors contribute equally to this work.

https://doi.org/10.1016/j.lfs.2019.116868
Received 24 July 2019; Received in revised form 3 September 2019; Accepted 10 September 2019
Available online 01 November 2019

However, whether could DEX affect histone demethylases, and how do the genome-wide epigenetic changes happen upon DEX treatment in sepsis are poorly explored.

In this study, we generate AKI mouse model induced by lipopolysaccharide (LPS) and additionally treated with DEX, CPI-455 (KDM5 inhibitor), KDM5A–IN–1 (KDM5A inhibitor) and PBIT (KDM5B inhibitor) respectively. We are trying to illustrate the regulatory relations between DEX and histone demethylases. Our results may provide more evidence for the epigenetic role of DEX in inflammatory control and sepsis treatment.

2. Materials and methods

2.1. Animal study

All procedures were performed in accordance with standard guidelines as described in the Guide for the Care and Use of Laboratory Animals (US National Institutes of Health 85–23, revised 1996). All animal protocols were agreed with the local Institutional Animal Care and Use Committee of Shandong University. Male C57BL/6 mice (Age: 6–8 week, weight: 34.2 ± 6.24 g, n = 30) purchased from SLAC Laboratory Animal Company (Shanghai, China) were maintained at 60.0 ± 10.0% humidity and 23.0 ± 2.0 °C under pathogen-free conditions. A standard diet and free drinking water were given for adaptive feeding more than 2 weeks before the experiment. Animals were randomly divided into 6 groups (5 mice in each group) including normal control (NC), AKI model (AKI), treatment of DEX (AKI + D), CPI-455 (KDM5 inhibitor) (AKI + C), KDM5A–IN–1 (KDM5A inhibitor) (AKI + K) and PBIT (KDM5B inhibitor) (AKI + P).

Initially, 25 μg/kg DEX (Sinopharm Chemical Reagent Co., Ltd, China) [8], 1 μmol/kg CPI-455 (GLPBIO, USA) [14], 20 μmol/kg KDM5A–IN–1 (MedChem Express, USA) [15] and 30 μmol/kg PBIT (Sigma, USA) [16] were intraperitoneally injected for 48 h in advance. The procedure of septic AKI model establishment was described previously [17]. In brief, LPS (5 mg/kg) was intraperitoneally injected to induce sepsis. An equal dose of PBS was administrated for the NC group. After 24 h, the blood samples and kidney tissues were isolated for the next experiments.

2.2. Enzyme linked immunosorbent assay (ELISA)

The levels of biochemical indicators in the serum were determined, including creatinine, mouse TNF-α, IL-8, calcitonin, C-reactive protein and endotoxin (Thermo, USA) in serum according to the manufacturer's instructions.

2.3. Chromatin immunoprecipitation assay

The ChIP assay was performed as previously described [18]. In brief, kidney tissues were removed capsule, and cut into small pieces in cold PBS, and added RIPA buffer (0.5% SDS) on ice for 30 min, then centrifuged at 13000 rpm for 15 min. The supernatant was harvested and treated by sonication to break genomic DNA into 200–500 bp. 10% were stored as input and the rest of supernatant was quantified the equal DNA concentration, then incubated with 1 μg IP grade antibodies of H3K4me3 (Activemotif, USA) 4 °C overnight. Protein-A beads were incubated next day at 4 °C for target protein pull down. The targeted or input DNA were directly used for PCR detection or constructed library for next generation sequencing. For ChIP-seq, template DNA was repaired to 3′-dA overhang and added the ligated adapter. The DNA library was eliminated the unligated adapters and selected the appropriate size for sequence using an Illumina Hiseq X Ten platform. The raw sequence reads were eliminated adaptors and low quality reads using Cutadapt and Trimmomatic [19], and checked the quality of clean reads using Fastqc [20]. The clean reads were mapped to the human genome (assembly hg38) using the Bowtie 2 algorithm [21]. Peaks ($p < 0.01$) were called by MACS 2 [22], and analyzed the different binding domains (FDR < 0.05), and annotated by DiffBind [23]. Gene ontology (GO) Analysis was used to interpret the biological function of the genes associated with differential peaks [24,25]. The peaks on certain genomic loci were visualized by Integrative Genomics Viewer (IGV). ChIP-seq data were deposited to ArrayExpress assigned with the accession number E-MTAB-8133.

2.4. Real-time PCR

Real-time quantitative PCR method was employed to detect the expression of target genes. Kidney tissues added 1 ml Trizol were squashed within liquid nitrogen, and 200 μl chloroform were added and vortexed for 15 s followed by 13000 rpm centrifuge at 4 °C. The upper supernatant was transferred to a new tube and added the same volume of isopropanol with 15 s vortex. The precipitation was washed by pure and 75% ethanol, then dissolved in the appropriate volume of DEPC water. First-Strand Synthesis System for reverse transcription (Thermo, USA) was used to synthesize cDNA from 1.5 μg total RNA according to the oligo (dT) version of the protocol. Real-time PCR was performed using CFX Fast real-time PCR system (Bio-Rad Laboratories, Inc., USA). The following cycle parameters were used for all experiments: 30 s at 94 °C for pre-denaturation, 20 s at 94 °C, 30 s at 60 °C, and 30 s at 72 °C for total 45 cycles. The relative levels of mRNA for each specific gene were normalized to GAPDH. Supplementary Table 1 shows the sequences for all primer sets used in these experiments.

2.5. Western blotting

Kidney tissues removed capsule were cut into small pieces, and treated with RIPA buffer (1% SDS) containing protease inhibitors. Then, the lysate was subjected to SDS-PAGE and transferred to PVDF membranes. The membrane was blocked with 5% fat-free milk in PBST for 30 min, followed by incubation overnight at 4 °C with final dilutions of primary antibodies against TNF-α, IL-8, histone H3, H3K4me1/2/3, H3K9me3, KDM5A/B/C, NF-κB signaling pathway associated proteins and GAPDH (CST, USA). After that, the membrane was washed 3 times and then incubated with HRP-conjugated secondary antibodies. The blotting bands were developed with ECL plus immunoblotting detection reagents (Thermo, USA), and captured using Image J.

2.6. Statistical analysis

The experimental data were processed with SPSS 20 software. One Way ANOVA was used for comparison of the difference among groups. p value less than 0.05 was considered as statistical significance.

3. Results

3.1. The change of overall H3K4me3 in renal cortex cells responding to DEX

Initially, the AKI mice model were prepared by LPS induction, and additionally treated with DEX, CPI-455, KDM5A–IN–1 or PBIT (treatment condition referring to “Materials and Methods”). The elevated inflammatory factors of TNF-α and IL-8 in serum and kidney of LPS treatment were determined an apparent septic model, which was consistent with the results of creatinine, calcitonin, C-reactive protein and endotoxin in serum (Fig. 1A and B). Moreover, the alleviation of DEX on effect of sepsis and kidney injury was observed, and the histone modification signals were determined a most pronounced change of H3K4me3 among NC, AKI and AKI + D groups (please check the grouping information in “Materials and Methods”) compared to H3K4me1/2 and H3K9me3 (Fig. 1C). Thus, H3K4me3 associated demethylases were inhibited via CPI-455 (KDM5 inhibitor), KDM5A–IN–1 (KDM5A inhibitor) and PBIT (KDM5B inhibitor) respectively to investigate the corresponding enzyme for H3K4me3 regulation. Although

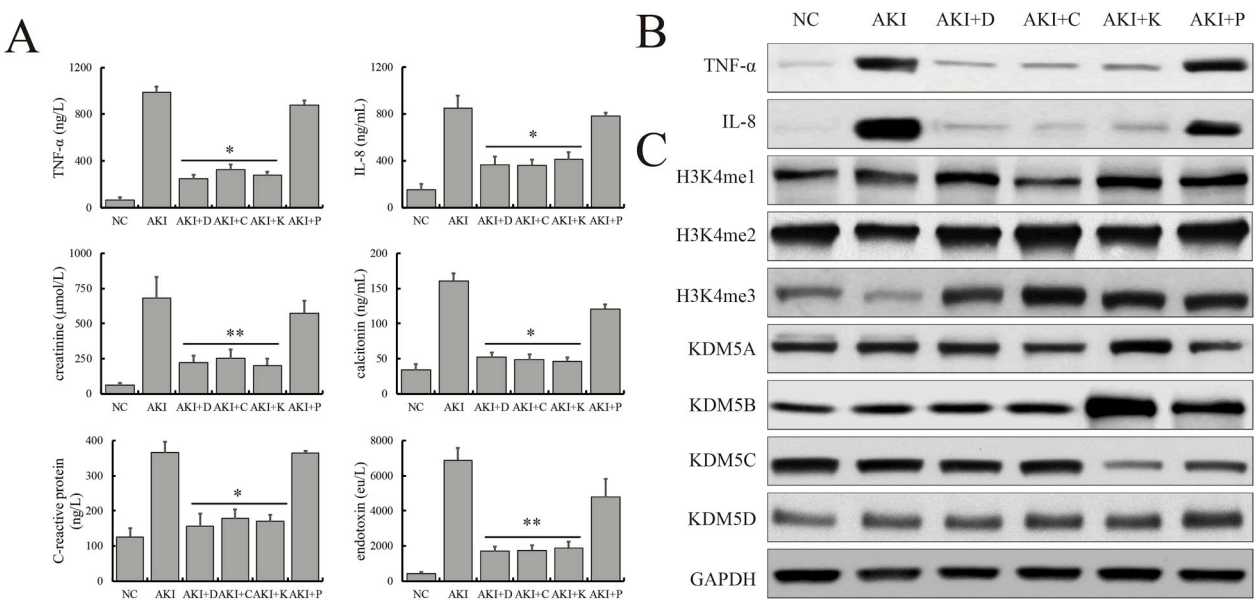

Fig. 1. The therapeutic effect of DEX on sepsis mediated AKI. The levels of the indicators including TNF-α, IL-8, creatinine, calcitonin, C-reaction protein and endotoxin in serum of AKI model treated by DEX and KDM5 family inhibitors (A). The protein levels of TNF-α, IL-8 (B), H3K4me1/2/3 and the histone lysine 4 demethylases KDM5A/B/C/D (C) in each group of AKI model treated by DEX and KDM5 family inhibitors. Experiments are conducted in triplicates. "*" and "**" represents *p* value less than 0.05 and 0.01 respectively.

the overall levels of H3K4me3 were all rescued in AKI + D, AKI + C, AKI + K and AKI + P groups compared to AKI group, the groups of AKI + D, AKI + C and AKI + K but not AKI + P showed a significantly effective therapy, which indicated that the specific selective targets regulated by KDM5A might contribute to AKI controlling. Taken together, the results above suggested that DEX attenuated sepsis-mediated renal failure via KDM5A inhibitor.

3.2. The genomic distribution of H3K4me3 upon DEX treatment

Since the groups of AKI + D could achieve the similar effect of AKI + C and AKI + K, which inhibited KDM5A on sepsis induced AKI, we questioned how KDM5A governed the H3K4me3 modification on the targeted genes regulated by DEX. ChIP-seq was employed to investigate the genomic H3K4me3 pattern in renal cortex tissues upon the treatment of DEX and KDM5A–IN–1. Approximately 103.7 M reads of AKI, 102.5 M reads of AKI + D and 103.2 M reads of AKI + K H3K4me3 sequencing data were produced respectively (Supplementary Table 2). The peak of H3K4me3 majorly distributed in promoter regions. We observed that the genomic enrichment of H3K4me3 was remarkably declined in AKI group compared to in AKI + D ($p = 0.037$) and AKI + K groups ($p = 0.014$) (Fig. 2A). Specifically, H3K4me3 enrichment of 4615 peaks (3964 genes) were up-regulated while 11958 peaks (5012 genes) were down-regulated in AKI + D (Fig. 2B) as well as 5494 peaks (3313 genes) were up-regulated while 2475 peaks (2010 genes) were down-regulated in AKI + K compared to AKI group were shown (Fig. 2C). The differential genes were intersected for the GO analysis and found a total up-regulated 269 peaks (190 genes) and down-regulated 805 peaks (598 genes) in AKI + D and AKI + K compared to AKI. Variety of genes associated with differential peaks such as MYD88, TLR4, NOS2, CASP3, PTGS2, TNF-α, CCL2, GSDMD were observed with higher H3K4me3 enrichment in AKI + D and AKI + K than AKI while ARPC2, GRTP1, YY1 and ZFP281 displayed a reversed tendency of H3K4me3 (Fig. 2D, Supplementary Table 3). These genes were studied gene ontology (GO) analysis and found that NF-κB, MAPK signaling pathways as well as the functions of inflammatory response and multiple metabolic processes were observed to be involved in DEX treatment (Fig. 2E). Taken together, our ChIP-seq data determined a potentially epigenetic role of DEX in gene transcriptional regulation against sepsis.

3.3. DEX-mediated inhibition of NF-κB to suppress KDM5A recruitment on target genes

Finally, we questioned how DEX affected KDM5A in sepsis. Since we noticed that NF-κB signaling pathway was related to DEX effect on AKI remission by GO analysis, which was also supported by the previous studies [26,27]. Thus, the protein levels of TLR4, MYD88, p-p65, p-IκBα as well as the location of p65 were investigated, and we observed that NF-κB pathway was activated in AKI group while suppressed in AKI + D and AKI + K groups (Fig. 3A and B). The occupancy of p65 and KDM5A on multiple genes were reduced in AKI + D compared to AKI group by ChIP-qPCR assay (Fig. 3C and D), which was also consistent with the transcription tendency of these target genes (Fig. 3E). In AKI + K group, the occupancy of p65 showed no significant difference from AKI group, which suggested that NF-κB was an up-stream signal for KDM5A regulation. Overall, our data determined that DEX could inhibit NF-κB signaling pathway to affect KDM5A recruitment on genomic DNA for protection from AKI in sepsis.

4. Discussion

As a type of α_2-adrenergic receptor agonist, DEX is determined to play a role in anxiolytic, sedative, and pain killing effects. Moreover, through the activation of α_7 nicotinic acetylcholine receptor receptors (nAChR), DEX can restrain the expression of cytokines, thereby inhibits inflammation and oxidative stress, rendering it beneficial effect on the systemic reaction of sepsis and multiple organ failure [28]. DEX can suppress a variety of signaling pathways, such as nAChR [6], GSK-3β/Nrf2 [29], TLR4/MyD88/NF-κB/iNOS [26], RAGE [30]. Once the genetic transcription activity triggered by these pathways, the concomitant epigenetic change, however is less investigated. Previous studies determined that DEX could increase acetylation through HDAC inhibition [7,31–33]. Similar with histone acetylation, H3K4me3, as another hallmark of transcription activation, was reported to play a synergy with acetylation at the same amino acid of histone 3 [34]. Since DEX could affect histone acetylation accumulation, however, how DEX regulated other epigenetic modifications was unknown. Thus, the

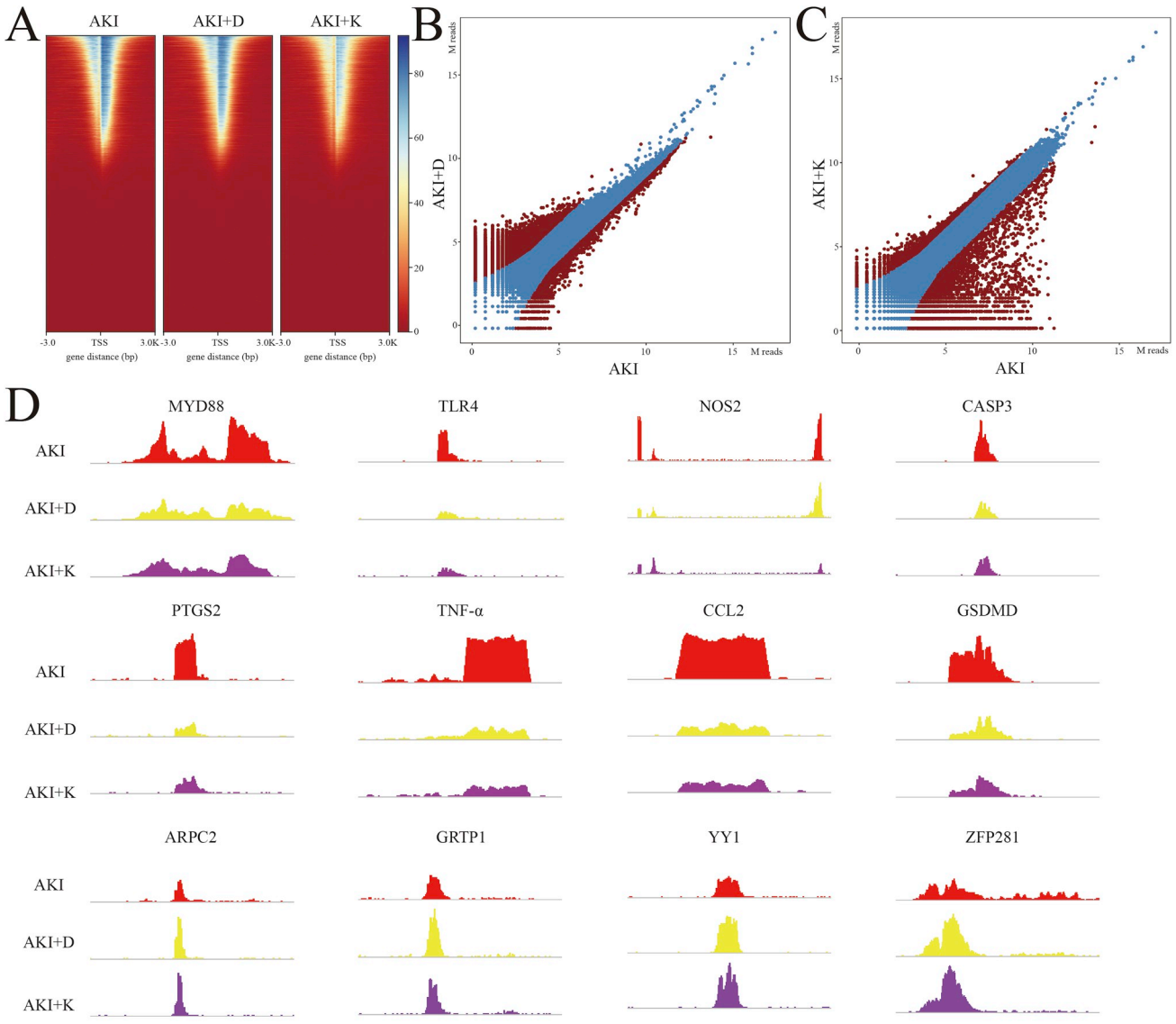

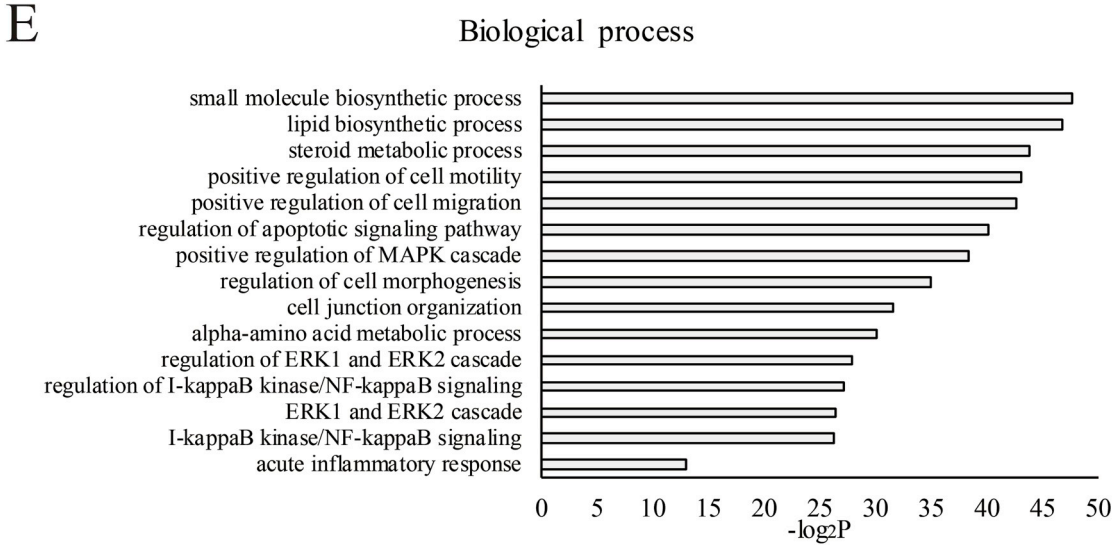

(caption on next page)

Fig. 2. The genomic enrichment of H3K4me3 in renal cortex tissues treated by DEX. The heatmap representation of H3K4me3 at all annotated gene promoters in renal cortex tissues of AKI, AKI + D and AKI + K models determined by ChIP-seq. Average enrichment measured by log2 (peak *p* values) in 200-bp bins is shown within genomic regions covering 3 kb up- and downstream of TSSs (A). The volcano representation of the different peaks compared between AKI and AKI + D (B) or AKI + K (C). Each brown spot mean a significantly different peak, while blue spot mean the peaks without statistical significance. Examples of the H3K4me3 enrichment patterns of eight genes including MYD88, TLR4, NOS2, CASP3, PTGS2, TNF-α, CCL2 and GSDMD in AKI (red), AKI + D (yellow) and AKI + K (purple) models. ChIP-seq data are shown in reads per million with the y-axis floor set to 0.5 reads per million. (For interpretation of the references to colour in this figure legend, the reader is referred to the Web version of this article.)

genome-wide pattern of H3K4me3 was our goal to be investigated in DEX treated sepsis model in this study.

In our study, we observe that H3K4me3 but not H3K4me1/2 was obviously rescued by DEX treatment (Fig. 1C), which indicates that H3K4me3 strongly links with the effect of DEX for transcriptional regulation. Because H3K4ac is considered overlapping with H3K4me3 at promoters while H3K4me1/2 typically enrich along coding regions [33], and since histone acetylation is apparently affected by DEX, it is reasonable that H3K4me3 will also responds to DEX treatment. It is interesting that H3K4me1/2 have no change upon DEX treatment. We speculated that first, DEX mainly facilitates promoter regions activation to regulate gene transcription, but not functions on coding regions of certain genes, secondly, except for H3K4me1 only catalyzed by KDM5B, H3K4me2/3 can be all regulated by KDM5A-D [35], and the enzymes associated with H3K4me1/2 such as KDM5B/C/D may be not the targets of DEX. To figure out which histone demethylases contribute to H3K4me3 metabolism in this sepsis model treated by DEX, KDM5A–IN–1 is observed to substantially achieve the similar effect of DEX compared to other inhibitors although we fail to find the commercial inhibitors for each KDM5 family enzyme (Fig. 1C). For the moment, KDM5A rather than KDM5B/C/D is speculated as a putative enzyme affected by DEX, which may have the special target genes for inflammation and oxidative stress controlling.

Our ChIP-seq data show the patterns of genome-wide H3K4me3 of kidney tissues across DEX treatment in sepsis model. We find that the genes associated with the function on inflammation and NF-κB signaling pathway display a variational H3K4me3 enrichment (Fig. 2D and E). DEX and KDM5A–IN–1 can both enhance H3K4me3 enrichment at the similar clusters of target genes (Fig. 2D), which further determined that KDM5A is an important enzyme to regulate H3K4me3 responding upon sepsis. Finally, combined with multiple previous studies [36,37], DEX is determined to suppress NF-κB signaling pathway (Fig. 3A and B). However, unexpectedly we observe that the genomic binding of p65 protein overlap with KDM5A on most of the target genes

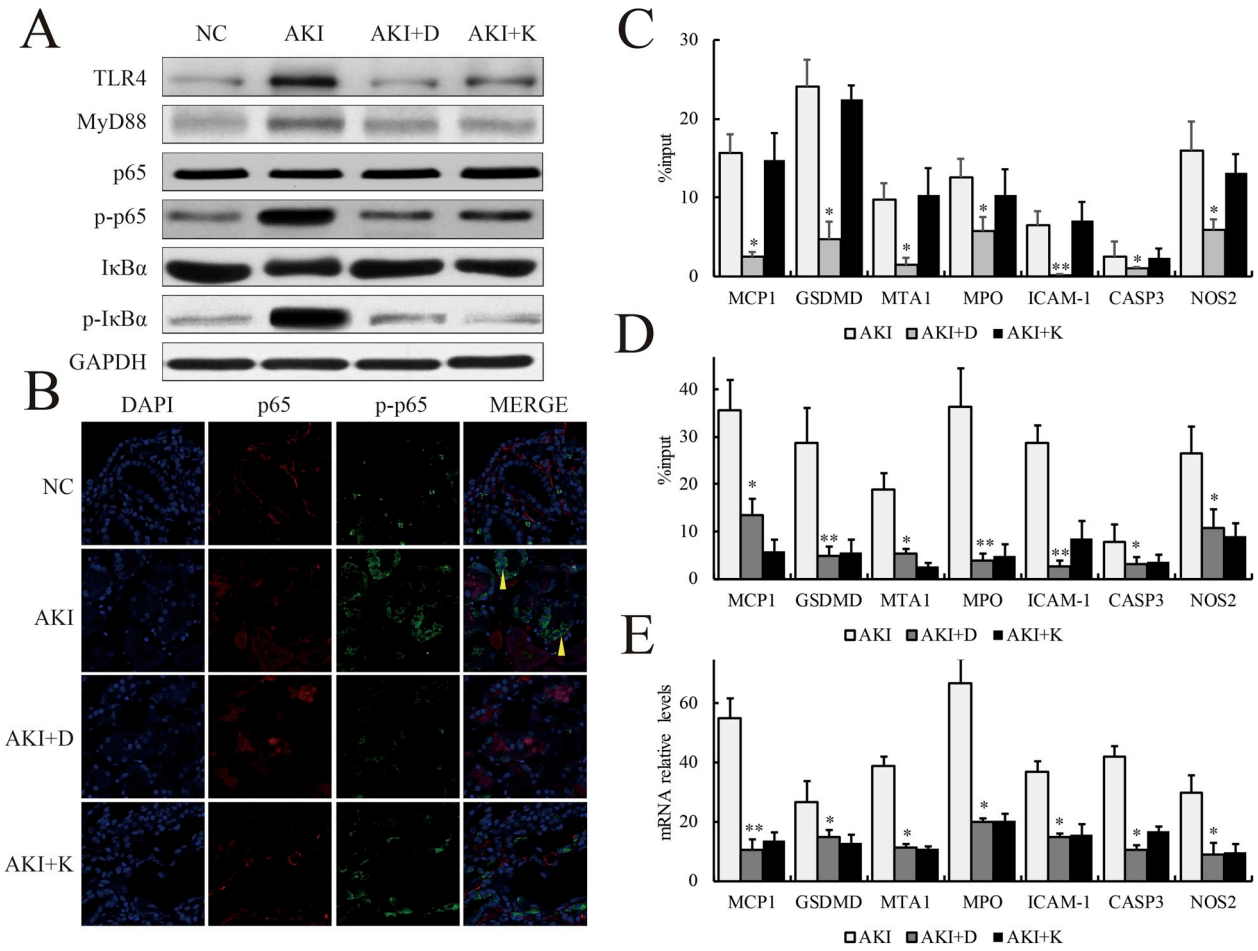

Fig. 3. The activity of NF-κB signaling pathway regulated by DEX. The protein expression of TLR4/MyD88/NF-κB in renal cortex tissues of AKI model treated by DEX and KDM5A inhibitor (A). The location of phosphorylated p65 in glomerulus of AKI model treated by DEX and KDM5A inhibitor (B). The occupancy of p65 (C), KDM5A (D) and the mRNA levels (E) of the targeted genes including MCP1, GSDMD, MTA1, MPO, ICAM-1, CASP3 and NOS2 in renal cortex tissues of AKI model treated by DEX and KDM5A inhibitor. The yellow arrows mark the enriched phosphorylated p65. Experiments are conducted in triplicates. "*" and "**" represents *p* value less than 0.05 and 0.01 respectively. (For interpretation of the references to colour in this figure legend, the reader is referred to the Web version of this article.)

affected by DEX (Fig. 3C). We speculate that the inactivated NF-κB pathway decrease the phosphorylated p65 entry into nucleus, and affect the recruitment of KDM5A to the target genes for H3K4me3 modulation.

Taken together, our results determine that DEX can effectively attenuate renal failure from sepsis via NF-κB mediated KDM5A inhibition.

Acknowledgements

This project is supported by WU JIEPING MEDICAL FOUNDATION (HRJJ20180733). L.Y. and Y.Y. performed the experiments and analyzed the data; J.Z. helped guiding experiments; C.W. designed the overall project, drafted and revised the manuscript. The authors declare no competing financial interests exist.

Appendix A. Supplementary data

Supplementary data to this article can be found online at https://doi.org/10.1016/j.lfs.2019.116868.

References

[1] K. Mantzarlis, V. Tsolaki, E. Zakynthinos, Role of oxidative stress and mitochondrial dysfunction in sepsis and potential therapies, Oxidative Med. Cell. Longev. 2017 (2017) 5985209.
[2] H.F. Galley, Oxidative stress and mitochondrial dysfunction in sepsis, Br. J. Anaesth. 107 (1) (2011) 57–64.
[3] D.S. Kriplani, C.B. Sethna, D.E. Leisman, J.B. Schneider, Acute kidney injury in neonates in the PICU. *Pediatric critical care medicine*, Pediatr. Crit. Care Med. 17 (4) (2016) e159–164.
[4] E.Y. Plotnikov, A.A. Brezgunova, I.B. Pevzner, L.D. Zorova, V.N. Manskikh, V.A. Popkov, D.N. Silachev, D.B. Zorov, Mechanisms of LPS-induced acute kidney injury in neonatal and adult rats, Antioxidants 7 (8) (2018).
[5] H.P. Shum, W.W. Yan, T.M. Chan, Recent knowledge on the pathophysiology of septic acute kidney injury: a narrative review, J. Crit. Care 31 (1) (2016) 82–89.
[6] K. Kang, Y. Gao, S.C. Wang, H.T. Liu, W.L. Kong, X. Zhang, R. Huang, Z.D. Qi, J.B. Zheng, J.D. Qu, et al., Dexmedetomidine protects against lipopolysaccharide-induced sepsis-associated acute kidney injury via an alpha7 nAChR-dependent pathway, Biomed. Pharmacother. 106 (2018) 210–216.
[7] C.H. Hsing, C.F. Lin, E. So, D.P. Sun, T.C. Chen, C.F. Li, C.H. Yeh, alpha2-Adrenoceptor agonist dexmedetomidine protects septic acute kidney injury through increasing BMP-7 and inhibiting HDAC2 and HDAC5, Am. J. Physiol. Renal. Physiol. 303 (10) (2012) F1443–F1453.
[8] Y.B. Sun, H. Zhao, D.L. Mu, W. Zhang, J. Cui, L. Wu, A. Alam, D.X. Wang, D. Ma, Dexmedetomidine inhibits astrocyte pyroptosis and subsequently protects the brain in in vitro and in vivo models of sepsis, Cell Death Dis. 10 (3) (2019) 167.
[9] Z. Luo, X. Qing, C. Benda, Z. Huang, M. Zhang, Y. Huang, H. Zhang, L. Wang, Y. Lai, C. Ward, Nuclear-cytoplasmic shuttling of class IIa histone deacetylases regulates somatic cell reprogramming, Cell Regen. 8 (1) (2019) 21–29.
[10] S. Samanta, Z. Zhou, S. Rajasingh, A. Panda, V. Sampath, J. Rajasingh, DNMT and HDAC inhibitors together abrogate endotoxemia mediated macrophage death by STAT3-JMJD3 signaling, Int. J. Biochem. Cell Biol. 102 (2018) 117–127.
[11] Y. Chen, Z. Liu, T. Pan, E. Chen, E. Mao, Y. Chen, R. Tan, X. Wang, R. Tian, J. Liu, et al., JMJD3 is involved in neutrophil membrane proteinase 3 overexpression during the hyperinflammatory response in early sepsis, Int. Immunopharmacol. 59 (2018) 40–46.
[12] D. Kim, H.J. Nam, W. Lee, H.Y. Yim, J.Y. Ahn, S.W. Park, H.R. Shin, R. Yu, K.J. Won, J.S. Bae, et al., PKCalpha-LSD1-NF-kappaB-Signaling cascade is crucial for epigenetic control of the inflammatory response, Mol. Cell 69 (3) (2018) 398–411 e396.
[13] J. Wang, K. Saijo, D. Skola, C. Jin, Q. Ma, D. Merkurjev, C.K. Glass, M.G. Rosenfeld, Histone demethylase LSD1 regulates hematopoietic stem cells homeostasis and protects from death by endotoxic shock, Proc. Natl. Acad. Sci. U. S. A. 115 (2) (2018) E244–E252.
[14] M. Vinogradova, V.S. Gehling, A. Gustafson, S. Arora, C.A. Tindell, C. Wilson, K.E. Williamson, G.D. Guler, P. Gangurde, W. Manieri, et al., An inhibitor of KDM5 demethylases reduces survival of drug-tolerant cancer cells, Nat. Chem. Biol. 12 (7) (2016) 531–538.
[15] Lai KW, Liang J, Zhang B, Labadie S, Ortwine D, Dragovich P, Kiefer J, Gehling VS, Harmange J-C: Pyrrolidine Amide Compounds as Histone Demethylase Inhibitors. In.: Google Patents; 2017.
[16] J. Sayegh, J. Cao, M.R. Zou, A. Morales, L.P. Blair, M. Norcia, D. Hoyer, A.J. Tackett, J.S. Merkel, Q. Yan, Identification of small molecule inhibitors of Jumonji AT-rich interactive domain 1B (JARID1B) histone demethylase by a sensitive high throughput screen, J. Biol. Chem. 288 (13) (2013) 9408–9417.
[17] H. Fan, Y. Zhao, J.H. Zhu, S-nitrosoglutathione protects lipopolysaccharide-induced acute kidney injury by inhibiting toll-like receptor 4-nuclear factor-kappaB signal pathway, J. Pharm. Pharmacol. (2019).
[18] P. Fei, W. Wang, S.H. Kim, S. Wang, T.F. Burns, J.K. Sax, M. Buzzai, D.T. Dicker, W.G. McKenna, E.J. Bernhard, et al., Bnip3L is induced by p53 under hypoxia, and its knockdown promotes tumor growth, Cancer Cell 6 (6) (2004) 597–609.
[19] A.M. Bolger, M. Lohse, B. Usadel, Trimmomatic: a flexible trimmer for Illumina sequence data, Bioinformatics 30 (15) (2014) 2114–2120.
[20] S. Andrews, FastQC A Quality Control Tool for High Throughput Sequence Data, (2013).
[21] B. Langmead, S.L. Salzberg, Fast gapped-read alignment with Bowtie 2, Nat. Methods 9 (4) (2012) 357–359.
[22] Y. Zhang, T. Liu, C.A. Meyer, J. Eeckhoute, D.S. Johnson, B.E. Bernstein, C. Nusbaum, R.M. Myers, M. Brown, W. Li, et al., Model-based analysis of ChIP-seq (MACS), Genome Biol. 9 (9) (2008) R137.
[23] C.S. Ross-Innes, R. Stark, A.E. Teschendorff, K.A. Holmes, H.R. Ali, M.J. Dunning, G.D. Brown, O. Gojis, I.O. Ellis, A.R. Green, et al., Differential oestrogen receptor binding is associated with clinical outcome in breast cancer, Nature 481 (7381) (2012) 389–393.
[24] A. Subramanian, P. Tamayo, V.K. Mootha, S. Mukherjee, B.L. Ebert, M.A. Gillette, A. Paulovich, S.L. Pomeroy, T.R. Golub, E.S. Lander, et al., Gene set enrichment analysis: a knowledge-based approach for interpreting genome-wide expression profiles, Proc. Natl. Acad. Sci. U. S. A. 102 (43) (2005) 15545–15550.
[25] H. Kong, P. Tong, X. Zhao, J. Sun, H. Li, CAsubtype: an R package to identify gene sets predictive of cancer subtypes and clinical outcomes, Interdiscip. Sci. 10 (1) (2018) 169–175.
[26] Y.H. Jin, Z.T. Li, H. Chen, X.Q. Jiang, Y.Y. Zhang, F. Wu, Effect of dexmedetomidine on kidney injury in sepsis rats through TLR4/MyD88/NF-kappaB/iNOS signaling pathway, Eur. Rev. Med. Pharmacol. Sci. 23 (11) (2019) 5020–5025.
[27] J. Zhang, Z. Wang, Y. Wang, G. Zhou, H. Li, The effect of dexmedetomidine on inflammatory response of septic rats, BMC Anesthesiol. 15 (2015) 68.
[28] I. Dardalas, E. Stamoula, P. Rigopoulos, F. Malliou, G. Tsaousi, Z. Aidoni, V. Grosomanidis, A. Milonas, G. Papazisis, D. Kouvelas, et al., Dexmedetomidine effects in different experimental sepsis in vivo models, Eur. J. Pharmacol. 856 (2019) 172401.
[29] X. Feng, W. Guan, Y. Zhao, C. Wang, M. Song, Y. Yao, T. Yang, H. Fan, Dexmedetomidine ameliorates lipopolysaccharide-induced acute kidney injury in rats by inhibiting inflammation and oxidative stress via the GSK-3beta/Nrf2 signaling pathway, J. Cell. Physiol. (2019).
[30] H. Hu, D. Shi, C. Hu, X. Yuan, J. Zhang, H. Sun, Dexmedetomidine mitigates CLP-stimulated acute lung injury via restraining the RAGE pathway, Am. J. Transl. Res. 9 (12) (2017) 5245–5258.
[31] Y. Wang, A. Jia, W. Ma, Dexmedetomidine attenuates the toxicity of beta amyloid on neurons and astrocytes by increasing BDNF production under the regulation of HDAC2 and HDAC5, Mol. Med. Rep. 19 (1) (2019) 533–540.
[32] S.P. Hu, J.J. Zhao, W.X. Wang, Y. Liu, H.F. Wu, C. Chen, L. Yu, J.B. Gui, Dexmedetomidine increases acetylation level of histone through ERK1/2 pathway in dopamine neuron, Hum. Exp. Toxicol. 36 (5) (2017) 474–482.
[33] B. Guillemette, P. Drogaris, H.H. Lin, H. Armstrong, K. Hiragami-Hamada, A. Imhof, E. Bonneil, P. Thibault, A. Verreault, R.J. Festenstein, H3 lysine 4 is acetylated at active gene promoters and is regulated by H3 lysine 4 methylation, PLoS Genet. 7 (3) (2011) e1001354.
[34] A. Lusser, Acetylated, methylated, remodeled: chromatin states for gene regulation, Curr. Opin. Plant Biol. 5 (5) (2002) 437–443.
[35] M. Pinskaya, A. Morillon, Histone H3 lysine 4 di-methylation: a novel mark for transcriptional fidelity? Epigenetics 4 (5) (2009) 302–306.
[36] L. Meng, L. Li, S. Lu, K. Li, Z. Su, Y. Wang, X. Fan, X. Li, G. Zhao, The protective effect of dexmedetomidine on LPS-induced acute lung injury through the HMGB1-mediated TLR4/NF-kappaB and PI3K/Akt/mTOR pathways, Mol. Immunol. 94 (2018) 7–17.
[37] H. Zhang, J. Sha, X. Feng, X. Hu, Y. Chen, B. Li, H. Fan, Dexmedetomidine ameliorates LPS induced acute lung injury via GSK-3beta/STAT3-NF-kappaB signaling pathway in rats, Int. Immunopharmacol. 74 (2019) 105717.